Prediction of the Mechanical Properties of a Crosslinking Polymer from a Combination of the Measured Kinetics and a Model for Network Growth

M. CLAYBOURN and M. READING*

Research Department, ICI Paints, Wexham Road, Slough, SL2 5DS, United Kingdom

SYNOPSIS

The mechanical properties of a crosslinking isocyanate–hydroxy system were predicted by a combination of the measured curing kinetics and a model for polymer network growth. The kinetic parameters were determined from FTIR using the linear rising temperature method (the activation energy = 52 kJ/mol, reaction order = 2.9). This data, combined with the network model, was used to predict the rise in elastic modulus as measured by dynamic mechanical analysis (DMA). The agreement between the predicted and experimental results was excellent over the early part of the curing, but the model failed at higher isocyanate conversions. In addition a novel method for obtaining the activation energy for the reaction directly from DMA results is presented; the value obtained from this method was in excellent agreement with that obtained by FTIR.

INTRODUCTION

The characterization of the cure behavior of coating materials and how it changes with variables such as temperature and formulation provides an essential base for developing models to describe film formation.[1] We propose that characterization data can be used with mathematical models for reaction kinetics and network buildup to give insights into the fundamental behavior of crosslinking systems and, ultimately, provide a predictive tool. The system considered here is based on a crosslinking reaction between isocyanate and hydroxyl functional resins[2,3] following the simple process

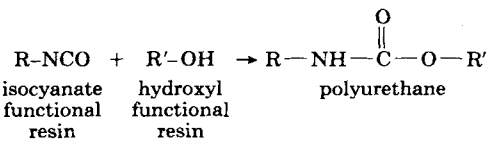

to form a durable polyurethane film. In real coating systems, both reactants are usually multifunctional, and the alcohol may have both primary and secondary —OH groups. The resulting film is often highly crosslinked to give high performance clear-coat finishes, for example, on car bodies.

The curing mechanism is an important consideration in understanding and, hence, predicting the behavior of these films. The approach taken here is to obtain kinetic parameters using a spectroscopic technique and to attempt to relate this to changes in physical properties such as viscosity or modulus using a model for network growth.

Time-resolved Fourier transform infrared spectroscopy (FTIR) provides an ideal technique for following the cure process and obtaining the kinetic parameters. The isocyanate infrared absorption band occurs in a clear spectral region and can be monitored without interference from other bands. By integrating this peak as a function of time, an accurate measure of the extent of reaction, α, during cure can be made.

For an isothermal experiment, where the extent of reaction, α, is monitored with time, the kinetic behavior for an nth-order reaction can be described by the relation

$$\frac{d\alpha}{dt} = k(1 - \alpha)^n \qquad (1)$$

* To whom correspondence should be addressed.

Journal of Applied Polymer Science, Vol. 44, 565–575 (1992)
 CCC 0021-8995/92/040565-11$04.00

where k is the rate constant. Assuming k is thermally activated and follows a simple Arrhenius expression over the temperature region of interest:

$$k = A \exp(-E/RT) \tag{2}$$

then the kinetic parameters, namely, the activation energy (E), preexponential factor (A), and n can be determined by a series of isothermal measurements at different temperatures. However, one of the main problems associated with this type of measurement on polymer systems is the intervention of the glass transition temperature (T_g), which increases as the reaction proceeds and can rise to meet the isothermal cure temperature. When this occurs, the reaction rate will be sharply reduced and the underlying kinetic behavior of the chemical process will be difficult to extract. This problem is particularly acute when dealing with low or ambient temperature isothermal cures. For temperatures significantly above ambient, there is also the difficulty of attaining rapid thermal equilibrium at the required temperature; this must be achieved if meaningful kinetic data are to be obtained using isothermal experiments.

Nonisothermal or temperature scanning measurements of film curing processes can overcome these experimental problems. Techniques such as dynamic mechanical analysis (DMA), differential scanning calorimetry (DSC), and FTIR can provide a means for obtaining information on the kinetics of cure using temperature scanning methods.[1,4-7] The effect of T_g can be avoided so long as the experimental temperature is always held above the T_g of the curing system. The kinetic parameters of a cure reaction can be obtained using a simplex minimization method applied to a single FTIR or DSC rising temperature scan.[8,9] Although this approach can often give good results when applied to polymer reactions, we have preferred to adopt a multiple heating rate method as it makes fewer assumptions and is generally more robust.[10] Also, its application to the FTIR results provides a useful parallel to the method we propose for the interpretation of DMA data where kinetic analysis of a single rising temperature experiment would be inappropriate.

We have developed an approach that combines the kinetic parameters from nonisothermal measurements with a simple model for polymer network growth and simple rubber elasticity theory with the result that we can predict the rise in elastic modulus as measured by DMA. This enables us to predict the behavior of coating materials from their formulation under different curing conditions.

THEORY

A convenient way of analyzing isothermal data is the reduced time plot.[11] If we write

$$f(\alpha) = (1 - \alpha)^n \tag{3}$$

and

$$g(\alpha) = \int_0^\alpha \frac{d\alpha}{f(\alpha)} \tag{4}$$

From Eqs. (1) and (4)

$$g(\alpha) = k \int_{t_0}^{t_\alpha} dt = kt \tag{5}$$

thus,

$$\frac{g(\alpha)}{g(0.5)} = \frac{t}{t_{0.5}} \tag{6}$$

where $g(0.5)$ is the value of $g(\alpha)$ at $\alpha = 0.5$ while $t_{0.5}$ is the time elapsed from the start of the experiment to when $\alpha = 0.5$. The interest of this expression lies in the fact that by plotting α against reduced time ($t/t_{0.5}$) the same shape is obtained regardless of the value of the rate constant, and thus independent of temperature. In this way, by co-plotting results, data from different experiments can be compared. Unless the behavior is the same at different temperatures, the activation energy cannot be determined as the assumption underlying Eqs. (1) and (2) are violated. For nth-order kinetics then

$$g(\alpha) = \frac{[1 - (1 - \alpha)^{(1-n)}]}{1 - n} \tag{7}$$

The experimental curve is compared with the computed reduced time plot to obtain the reaction order. The value of k at each temperature can then be found by plotting $g(\alpha)$ against t once the reaction order has been determined and shown to be independent of temperature. A and E values can then be determined from an Arrhenius plot of $\ln(k)$ against $1/T$.

To obtain the kinetic parameters from the rising temperature FTIR results, we have used a method based on the analysis of a series of experiments performed at different heating rates. For this nonisothermal technique, the kinetic behavior is modeled using an Arrhenius-type expression based on Eqs. (1) and (2):

$$\frac{d\alpha}{dT} = \frac{(1-\alpha)^n}{b} A \exp\left(-\frac{E}{RT}\right) \tag{8}$$

where $b = dT/dt$, i.e., the heating rate. It can be shown that for a rising temperature experiment[12]

$$g(\alpha) = \frac{AR}{bE} T^2 e^{-E/RT} I(E, T) \tag{9}$$

where

$$I(E, T) = 1 - \frac{2!}{E/RT} + \frac{3!}{(E/RT)^2} - \frac{4!}{(E/RT)^3} + \cdots \tag{10}$$

Equation (9) can be rearranged to give

$$\ln \frac{b}{T^2 I(E, T)} = \ln \frac{AR}{Eg(\alpha)} - \frac{E}{RT} \tag{11}$$

Using the approximation proposed by Doyle,[13-15] Eq. (11) can be reduced to the simple form for a given extent of reaction, α:

$$\ln(b) = X - 1.0516 \frac{E}{RT_b(\alpha)} \tag{12}$$

where X is a constant. This is effectively a modified form of the approach proposed by Ozawa.[16] A series of experiments is carried out at different heating rates, b, and the temperature at which a given extent of reaction is reached [$T_b(\alpha)$] is determined for each experiment. The extent of reaction can be measured directly by FTIR or inferred from the DMA results (see later for detailed explanation). A plot of $\ln(b)$ against $1/T_b(\alpha)$ from these results gives a value for the activation energy. This will be true regardless of the form of $g(\alpha)$. The Doyle approximation has to be treated with some caution. However, here it is only used as the starting point for a subsequent iterative treatment that takes the Taylor series in Eq. (11) to four terms (see later).

We offer a novel extension to this approach for application to DMA data. To do this we must consider a polymer impregnated onto a glass fiber braid being sheared at a frequency of 1 Hz. The polymer is applied to the braid in an uncured form; then a temperature scanning experiment is started. The polymer crosslinks and the dynamic modulus measured by the DMA increases. To analyze this type of data, we must make some assumptions; the first assumption is that the dynamic storage modulus G' of the polymer measured at 1 Hz is proportional to the static modulus G, which can be calculated from elementary rubber elasticity theory. Therefore, for a polymer denoted p,

$$G'_p = \text{constant} \times G_p \tag{13}$$

where G_p is the static shear modulus of the polymer. Provided the experimental temperature is above the T_g of the polymer measured at 1 Hz, this is likely to be a good assumption as the sample must be in the rubbery plateau region in both the frequency and temperature domains. The impregnated glass fiber braid is effectively a polymer–fiber composite. Taking the treatment of Nielson,[17] the experimental configuration used requires the expression for longitudinal-tranverse shear modulus:

$$\frac{G_c}{G_p} = \frac{1 + B}{1 - Ba} \tag{14}$$

where G_c is the shear modulus of the composite, a is a constant related to the packing fraction of the fibers of the braid and the type of packing and

$$B = \frac{E_g/E_p - 1}{E_g/E_p + 1} \tag{15}$$

where E_g is the tensile modulus of the glass and E_p is the tensile modulus of the polymer. During the experiment the polymer is always above its T_g. The rubbery modulus of the system considered here is at least two orders of magnitude below that of the glass; thus, it is a good approximation to say that $B = 1$. It can be seen that

$$G_p = \text{constant} \times G_c \tag{16}$$

From elementary rubber elasticity theory

$$G = \frac{dR\,T}{M_c} \tag{17}$$

where G is the shear modulus, d is the sample density, R is the gas constant, T is absolute temperature, and M_c is the average weight between crosslinks. While this expression is based on a very simple model of rubber elasticity that neglects, for example, entanglement effects, it has been shown to be an adequate first approximation in many cases.[18] In the

temperature region of interest we shall assume that mass is not lost and so

$$G_p = \text{constant} \times \frac{T}{M_c} \tag{18}$$

It should be pointed out that this is only true for the "rubbery" plateau above the T_g. From Eqs. (13), (16), and (18) we can write

$$\frac{1}{M_c} = \text{constant} \times \frac{G_c'}{T} \tag{19}$$

where G_c' is the measured dynamic storage modulus of the composite; $1/M_c$ can be taken as a measure of extent of reaction. Thus, if a series of DMA experiments are carried out at different heating rates and a value of G'/T is chosen in each one, then Eq. (12) can be used to determine the activation energy by exact analogy with the procedure described for the FTIR results.

The crosslinking reaction, which leads to gelation and the buildup of a network, can be modeled using various methods. The approach used here was originally proposed by Macosko and Miller;[19] given the average molecular weight and relative quantities of the reacting species, then the gel point, sol fraction, pendant fraction, elastically effective weight fraction, and crosslink density can be determined as a function of extent of reaction.

The methods given can be used to determine a function that describes extent of reaction as a function of time and temperature. The expressions derived by Miller enable crosslink density to be calculated as a function of extent of reaction. The two are combined to predict crosslink density as a function of time and temperature.

EXPERIMENTAL

The example used in this analysis is a standard two-pack coating system consisting of a tri-functional isocyanate crosslinker and a hydroxy functional acrylic resin composed of secondary —OH groups with a small proportion of primary —OH groups. The reaction follows the simple process described in the introduction with the product being a polyurethane.

A Bruker IFS48 FTIR spectrometer was used to follow the curing reaction both isothermally and nonisothermally. The —NCO and —OH components were mixed in a stoichiometric ratio with catalyst and coated onto a KBr disc. This was mounted onto a Specac variable temperature cell that has a linear temperature programmer for controlled sample heating. The cure process was monitored by the decay of the —NCO band at 2275 cm^{-1} both isothermally and at different heating rates. Figure 1 shows a typical decay in the —NCO stretching frequency as measured by FTIR for a temperature ramping method with a heating rate of 0.5°C/min. The extent of reaction, α, during cure was determined from the FTIR results by integration of the isocyanate band at 2275 cm^{-1} and normalizing against the initial peak area so that

$$\alpha = 1 - \frac{A_t}{A_{t=0}} \tag{20}$$

The DMA measurements were carried out on a Du Pont 983 DMA with the sample supported on a glass fiber braid in the shear mode. The samples were prepared and catalyst added just before impregnating the braid (25 μL were applied from a micropipette). Linear rising temperature experi-

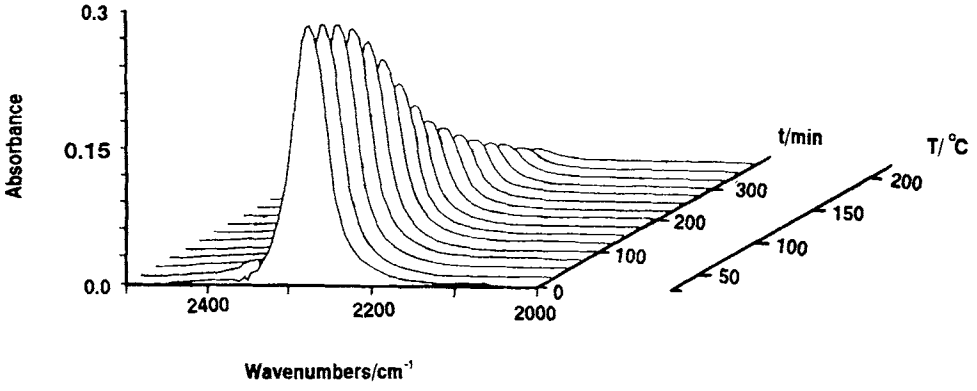

Figure 1 Decay of the isocyanate IR absorption band at a heating rate of 0.5°C/min.

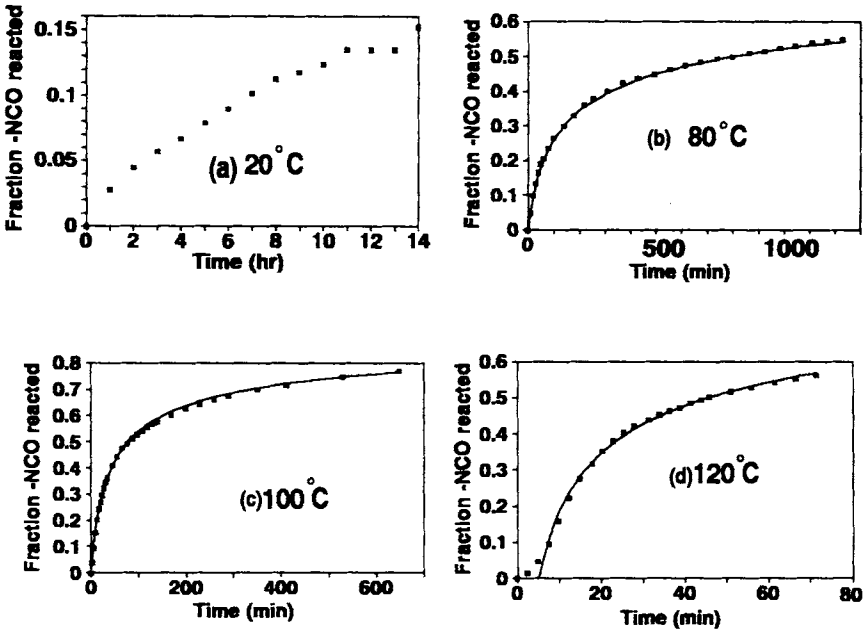

Figure 2 Isothermal cures at (a) 20, (b) 80, (c) 100, and (d) 120°C. The solid lines refer to reduced time fits to the data (see Table I).

ments were performed at the same rates as used for the FTIR measurements, namely, 0.5, 1.0, 2.0, 3.0, and 5.0°C/min. All experiments were performed at a shear frequency of 1 Hz. The braid dimensions were 10 × 13 × 0.1 mm and the dynamic displacement was 0.2 mm.

The network model used was that proposed by Macosko and Miller[19] for a simple *AB* reaction. It enables systems comprising any number of *A* species with any combination of functionalities to be crosslinked with any number of *B* species with any combination of functionalities. It provides, before the gel point, average molecular weight and, after the gel point, crosslink density together with weight of pendant fraction and sol fraction. Here the hydroxy functional polymer was denoted as the *A* species while the isocyanate was the *B* species.

RESULTS AND DISCUSSION

FTIR

Initially, isothermal measurements were performed to assess the applicability of this approach. Temperatures for these experiments were 25, 80, 100, and 120°C, and these results are given in Figure 2. At 25°C the reaction was very slow, and after 15 h the process had only gone to 15% completion. For each temperature, except 25°C where the extent of reaction was too low, the apparent order of reaction was calculated using the reduced time method.[11] The results are shown in Table I. The thermal lag in the system increased with increasing temperature as indicated by the acceleratory period for the 120°C experiment; for the reduced time analysis, a delay of 5 min before starting the reaction was estimated for this experiment.

If, for the reasons given in the introduction, an experimenter wants to measure reaction kinetics that are unaffected by the intervention of the T_g, then isothermal experiments must be conducted within a temperature "window." The lower boundary of this window is given by the T_g of the fully crosslinked material (or the highest T_g it can achieve in practice) while the upper boundary is its decomposition temperature. It is often the case for systems that must cure under ambient or low-bake conditions that the T_g of the fully crosslinked system is

Table I Orders of Reaction Using the Reduced Time Analysis on the Isothermal Data

Temperature (°C)	Order of Reaction (n)
25	No reasonable fit
80	5.7
100	3.6
120	4.0

relatively high compared to the normal cure temperature. This means that, within the temperature window, the reaction occurs very rapidly. Ideally, for an isothermal experiment, the sample should be heated instantaneously from some low temperature at which no reaction is occurring to some higher temperature. Clearly this is not achievable in practice and, in general, the higher the temperature is above ambient, the more difficult it will be to approach ideal behavior. The important consideration is the speed with which the sample can be brought to the desired temperature compared with the rate of the chemical reaction. It can be seen, therefore, that we have particularly acute experimental difficulties: high reaction rates, and relatively elevated temperatures. For the FTIR experiments there is the added practical problem of rapidly and uniformly heating a KBr disc. These difficulties are well illustrated by our isothermal results. At 100°C or below the reaction order is very high, 3.6 or above, strongly suggesting a diffusion-limited process, i.e., one impeded by the rise of the T_g to meet the cure temperature. At 120°C the thermal lag, which is not significant on the time scale of the reaction at the lower temperatures, becomes clearly evident and starts distorting the results. In fact, DMA results presented later show that even at this temperature the sample is not on the rubbery plateau of the system when cured to its maximum attainable crosslink density (see Fig. 8). The rubbery plateau is only achieved above 130°C. Thus, these results are entirely consistent with glass transition data given later.

The alternative method that may eliminate the influence of the T_g on the kinetics is the rising temperature experiment; ideally, the increasing experimental temperature remains sufficiently well above the T_g of the system to prevent it from having any effect while enabling the reaction to begin at lower

Table II Activation Energies Calculated Using the Doyle Approximation

Extent of Reaction (α)	Energy (kJ/mol)
0.1	54 ± 2
0.2	54 ± 3
0.3	53 ± 3
0.4	52 ± 3
0.5	50 ± 4
0.6	49 ± 5
0.7	50 ± 9

From Refs. 13–15.

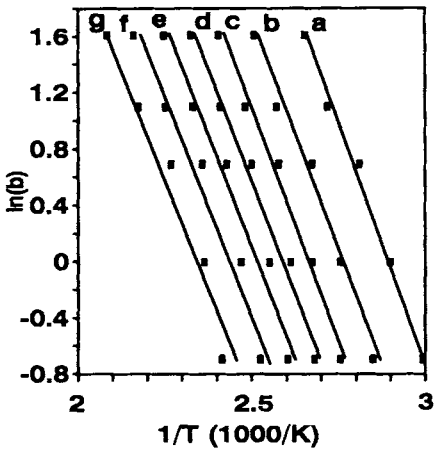

Figure 3 Arrhenius plots for the different heating rates at different extents of reactions: (a) 0.1, (b) 0.2, (c) 0.3, (d) 0.4, (e) 0.5, (f) 0.6, and (g) 0.7.

temperatures. In addition, by taking $T(0) = 25°C$, thermal lag and resulting experimental errors can be avoided. Experiments were performed at heating rates of 0.5, 1, 2, 3, and 5°C/min. Using Eq. (12) (Doyle approximation) activation energies were calculated for the range of extents of reaction 0.1 to 0.7; the results are shown in Table II; the plots are given in Figure 3.

The close agreement between all of the values obtained at different extents of reaction indicates that the reaction is controlled by a single activation energy and the same $g(\alpha)$ applied in all cases. Thus the assumptions underlying the kinetic treatment adopted here are conformed to, and it appears that the T_g has had little influence on the reaction rate because the reaction temperature has been successfully maintained above the T_g at all times. The DMA data presented later provide further experimental confirmation of this point. The average value is 52 kJ/mol, and this gave an initial approximation for E. Having determined an initial approximation for the activation energy, it is comparatively simple to derive the kinetic parameters from the FTIR results using Eq. (7) together with Eq. (9). These equations were incorporated into a LOTUS spreadsheet together with the experimental α, T values. By carrying out an iterative procedure manually, values for n and A can quickly be arrived at that provide good agreement with the experimental data. This is illustrated in Figure 4, which shows plots of observed values against model values for the three heating rates, all of which show close agreement over almost the whole range of α. It also illustrates the α against T plots together with the model predictions—again

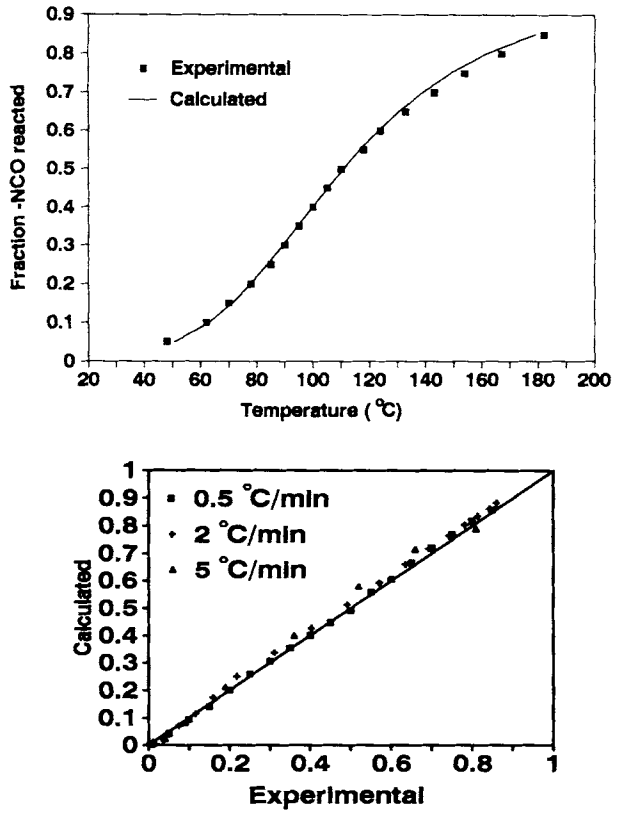

Figure 4 (a) Fit of the kinetic model given by Eq. (11) to the experimental data for a heating rate of 0.5°C/min. (b) Experimental data against calculated data [Eq. (11)] for heating rates of 0.5, 2, and 5°C/min.

the level of agreement is excellent. The expression derived in this way is as follows:

$$\frac{d\alpha}{dt} = (1 - \alpha)^{(2.9\pm0.1)}(6.6 \pm 0.4) \times 10^3 \exp\left[-\frac{(52 \pm 4) \times 10^5}{RT}\right] \quad (21)$$

It can be seen that, although the reaction order is considerably lower than any of the isothermal experiments, it does not have the expected value of 2 that a bimolecular reaction should have. However, this lowering and the fact that n is independent of b provide additional evidence that the T_g has not influenced the kinetics of the reaction. Overall, the results confirm that the nonisothermal approach is more reliable. If there was any influence of the T_g on the reaction rate, there would be significant deviations from the model particularly at the slowest heating rates. The high value for the order of reaction probably arises due to the fact that once the gel point has been passed and a dense network established, then diffusion eventually has a predominating influence on the reaction kinetics. Whatever the root cause, our data clearly shows that the reaction kinetics can be modeled using this expression on an empirical basis, over a wide range of temperature and extent of conversion. This is sufficient for the purposes of our analysis.

Dynamic Mechanical Analysis

The chemistry of the cure reaction results in a growing crosslinked network so that the mechanical properties of the curing system change with time. An analogous series of nonisothermal experiments at the same heating rates as those used for the FTIR measurements were performed by DMA. A typical result is shown in Figure 5; at time 0, the material was a low viscosity liquid so that dynamic storage modulus was initially zero. Further into the experiment the modulus underwent a rapid increase to a first maximum; then a slight decrease followed by a further rapid increase. At temperatures above the first maximum bond scissions were clearly occurring

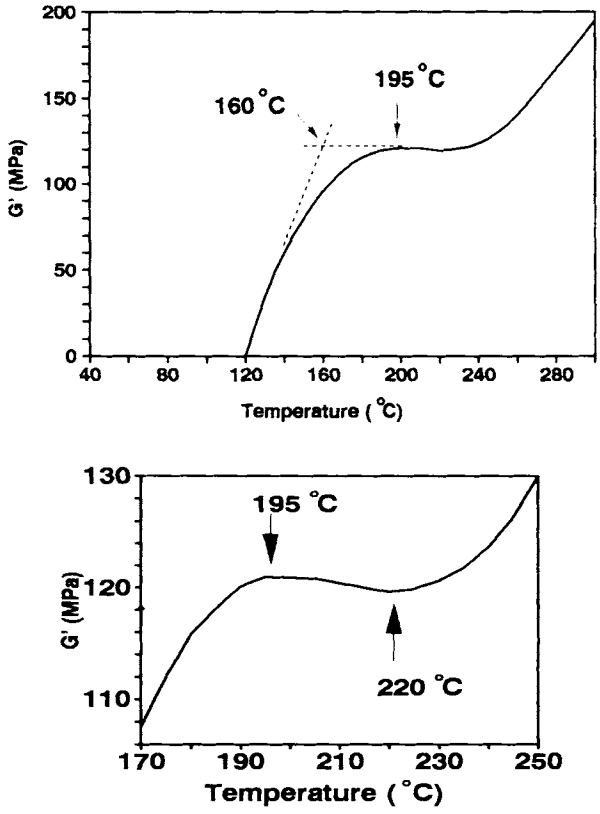

Figure 5 (a) DMA characteristic for the curing process for a heating rate of 5°C/min. (b) As (a) but expanded in the temperature region of the inflection.

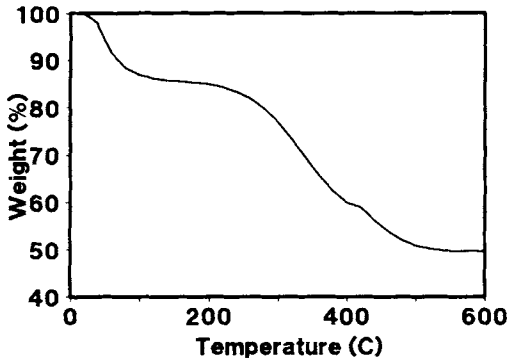

Figure 6 Behavior of the curing material on a glass fiber braid as monitored by TGA.

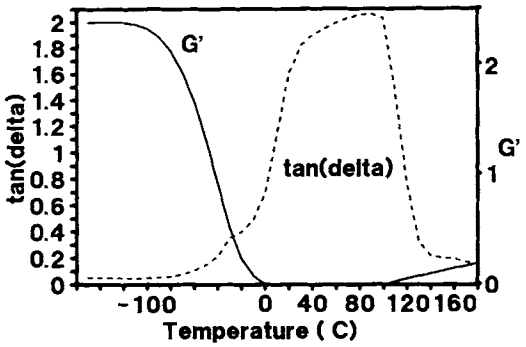

Figure 7 Behavior of the curing material as monitored by DMA at a heating rate of 5°C/min.

as the modulus decreased; the TGA result given in Figure 6 showed that the onset of decomposition was in this temperature region. The second increase was ascribed to carbonization of the sample as the TGA showed rapid weight loss. It should be noted that in the temperature region where the modulus was increasing rapidly there was very little weight change, thus the assumption of constant density made in the derivation is validated in the region of interest. The early mass loss shown in this plot is due to solvent evaporation. An advantage of the methods employed here is that they can be used to study coating systems where solvent loss occurs.

The change in T_g during the course of the reaction was investigated by rapidly cooling the sample to −100°C immediately after applying to the DMA braid, then scanning at 5°C/min up to 175°C, the temperature at which the maximum modulus was attained at this heating rate. The sample was cooled again and then heated to 200°C. The results from these two experiments are shown in Figures 7 and 8. The tan (delta) peak in Figure 7 is poorly resolved due to the fact that the liquid (uncrosslinked) polymer braid composite has a zero modulus immediately after the glass transition, and the signal to noise ratio is poor under these conditions. From these results it can be clearly seen that the T_g of the sample at the start of the experiment and at the point when the maximum modulus was obtained were both well below the sample temperature; and, therefore, the modulus measured was the rubbery modulus of the material. This confirms the inferences made from the kinetic data given earlier. Inspection of the results shows that this is also true even when the heating rate is reduced to 0.5°C/min. In addition it can be seen that an isothermal temperature of 100°C is within the transition region and even 120°C would not be in the rubbery plateau. This is consistent with the discussion of the isothermal results given earlier.

The activation energy for the cure reaction can be determined from the DMA results following the procedure outlined in the theory section. The data at all the heating rates, G'/T against T, were normalized as shown in Figure 9. The normalization is with respect to the initial maximum modulus observed. This is necessary because, although great care is taken in sample application on the braid, consistency is difficult, and absolute values for G' can vary from experiment to experiment. An analogous Arrhenius plot to that for FTIR (Fig. 3) was obtained—Figure 10 shows $\ln(b)$ vs. $1/T$ (at half maximum height in Fig. 9). The activation energy was found to be 53 ± 2 kJ/mol; this is consistent with the literature.[20,21] Considering the completely different experimental approaches used, the values obtained for the activation energy by FTIR and DMA are in excellent agreement. This further con-

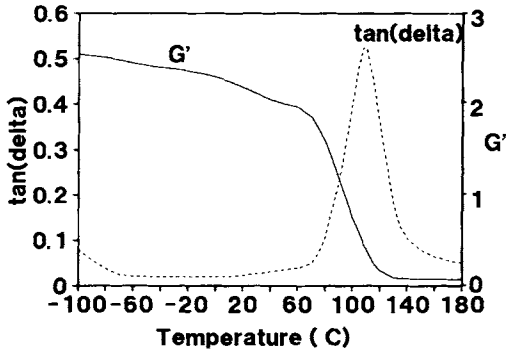

Figure 8 Monitor of the T_g of the cured material after heating to 175°C at 5°C/min.

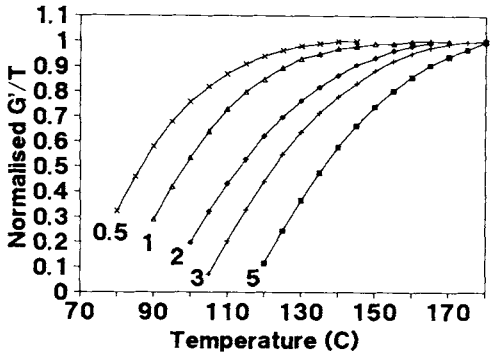

Figure 9 Normalized DMA results for different heating rates.

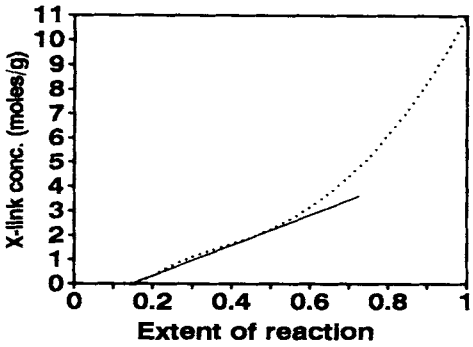

Figure 11 The calculated crosslink density as a function of the extent of reaction.

firms that the theoretical approach adopted here has some validity. It should be noted that this treatment assumes that the modulus maximum occurs at the same extent of reaction in each case. Inspection of the FTIR data and the closeness of the values obtained by the two different methods tend to support this assumption in this case. However, a more general treatment that avoids this assumption will be given in a future article.

Network Model

For a given extent of reaction, network models can be used to calculate the gel point, sol fraction, pendant fraction, elastically effective weight, and crosslink density. Using this information, M_c can be determined. The network model[19] was applied to a simple $A + B$ reaction. Figure 11 shows a plot of the crosslink density against extent of reaction as calculated from this model.

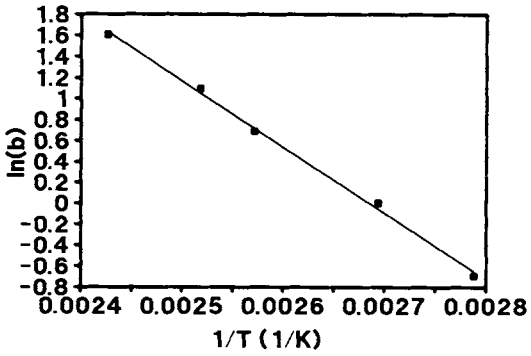

Figure 10 Arrhenius plot of the DMA results. The thermal activation energy of the cure process is 53 ± 2 kJ/mol.

We now have a method for calculating the extent of reaction as a function of time and temperature from the kinetic model obtained by FTIR nonisothermal measurements and also a means of calculating the elastic modulus as a function of extent of reaction from the Miller network model.

Using the network model, a value for M_c was calculated, and the theoretical modulus was normalized using the following expression derived from Eq. (19):

$$\text{Normalized } G' = \frac{T(\alpha)M_c(\min)}{T(\min)M_c(\alpha)}$$

where

$T(\alpha)$ = temperature at extent of react α
$M_c(\alpha)$ = M_c at extent of reaction α
$M_c(\min)$ = minimum M_c (at the G' maximum)
$T(\min)$ = temperature at $M_c(\min)$ (at the G' maximum)

Using these values of G' with the kinetic model allows theoretical normalized DMA profiles to be plotted for any given value of activation energy, reaction order, and preexponential factor for any AB system with varying functionality and composition.

Simple inspection of the results makes it clear that the maximum G' measured does not correspond to complete reaction. From Figure 9 it can be seen that the G' maximum occurs at 140°C at 0.5°C/min; inspection of Figure 4 shows this corresponds to approximately 68% reaction. In fact, it corresponds to about 65 ± 3% reaction in all cases. Moreover, according to the model, the modulus should continue to rise rapidly up to 65% reaction, whereas the ex-

perimental results clearly show a deceleratory period. In the absence of any absolute values, comparison between two normalized sets of data is necessarily somewhat arbitrary. We have chosen to adopt the following procedure; between an extent of reaction of about 0.15 (the gel point where G' begins to rise) and 0.6 (close to the extent of reaction at the maximum G'), the extent of reaction is approximately a linear function of temperature; see Figure 4. Also crosslink density is approximately a linear function of extent of reaction, see Figure 11. Thus crosslink density, and therefore G', should be approximately a linear function of temperature. Linear behavior is observed just after gelation. This was extrapolated to meet the line corresponding to the value of the first maximum in G' (see Fig. 5). This temperature corresponds to an extent of reaction of about 45% in all cases so the predicted modulus data from the model were normalized against the modulus at this extent of reaction. The argument behind this method is that this is the approximate course the modulus increase would have taken in this temperature region had ideal behavior been conformed to. The results are presented in Figure 12. It can be seen that the agreement is good over the early part of the cure. It should be noted that, while the normalization procedure influences the degree of agreement between the model and the experimental data over the later part of the cure, it cannot influence the prediction of the onset of modulus buildup. This aspect of the predicted behavior is in excellent agreement with experiment. The failure of the model at higher degrees of cure is probably due to the fact that, for this system, the distance between crosslinks is rapidly reduced to a few tens of monomer units; thus, the underlying assumptions of the rubbery elasticity expression used here are violated. It assumes that each chain is free to adopt a Gaussian distribution; when the chain length becomes too short, this assumption will not hold.

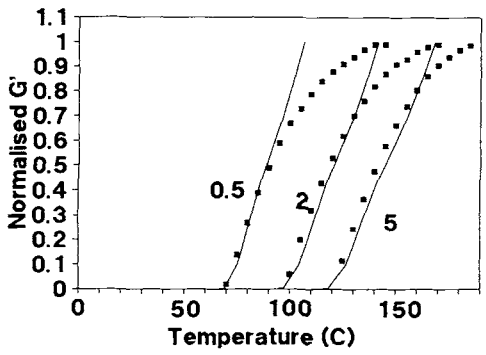

Fiugre 12 Plot showing the agreement between the predicted (solid lines) and the modulus measured by DMA for heating rates of 0.5, 2, and 5°C/min.

CONCLUSION

Kinetic parameters for a commercial polyurethane coating system were obtained from FTIR using a nonisothermal method. This data was coupled to a network model and simple rubber elasticity theory to give a prediction of the mechanical behavior of the curing system. The predictions of the model were compared with an independent set of experimental results obtained by DMA. While a number of assumptions were made and a normalization procedure was used rather than absolute values, the approach taken was successful over the early part of the cure, and this type of model will enable a more predictive approach for optimizing commercial formulations.

In addition, a method was devised to obtain activation energies directly from DMA data, and the value obtained using this method were in excellent agreement with those obtained from the FTIR results.

The authors would like to thank M. Sarkar for helpful discussions on network modeling and C. McDermot, M. Bahra, and R. Ryan for their contribution to the experimental work and data analysis. We would also like to thank D. Shakespeare for writing the LOTUS macro for the network model.

REFERENCES

1. T. Provder, *J. Coatings Tech.*, **61**, 32 (1989).
2. J. H. Saunders and K. C. Frisch, *Polyurethanes Chemistry and Technology*, Vol. I, Wiley-Interscience, Robert E. Krieger Publ. Co., Malabar, FL, 1962.
3. G. Oertel, Ed., *Polyurethane Handbook, Chemistry Raw Materials Processing, Application, Properties*, Hanser Publishers, Munich, 1985.
4. R. W. Snyder and C. Wade Sheen, *Appl. Spectrosc.*, **42**, 655 (1988).
5. G. M. Carlson and T. Provder, *Proc. Water-borne and High-Solids Coatings Symposium*, **12**, 44 (1985).
6. G. M. Carlson, C. M. Neag, C. Kuo, and T. Provder, *Polym. Preprints*, **25**, 171 (1984).
7. T. Provder, C. M. Neag, G. Carlson, C. Kuo, and R. M. Holsworth, *Anal. Calorim.*, **5**, 377 (1984).
8. M. E. Koehler, A. F. Kah, C. M. Neag, T. F. Niemann, F. B. Malihi, and T. Provder, *Anal. Calorim.*, **5**, 361 (1984).

9. G. M. Carlson and T. Provder, ACS Symposium Series No. 313, *Comp. Appl. Polym. Lab.,* 241 (1986).
10. M. Reading, D. Dollimore, J. Rouquerol, and F. Rouquerol, *J. Thermal Anal.,* **29,** 775 (1984).
11. J. H. Sharp, G. W. Brindley, and B. N. N. Achar, *J. Am. Ceram. Soc.,* **49,** 379 (1966).
12. R. Whitehead, D. Dollimore, D. Price, and N. S. Fatemi, *Proc. 2nd Europ Symp Thermal Analysis,* D. Dollimore, Ed., (Publ Heyden, Aberdeen), 1981, pp. 51–53.
13. C. D. Doyle, *J. Appl. Polym. Sci.,* **6,** 639 (1962).
14. C. D. Doyle, *Nature (London),* **207,** 290 (1965).
15. C. H. Bamford and C. F. H. Tipper, Eds., *Reactions in the Solid State,* Vol. 22, Elsevier Publishing, Amsterdam, 1980, p. 103.
16. T. Ozawa, *J. Thermal Anal.,* **2,** 301 (1970).
17. L. E. Nielsen, *Mechanical Properties of Polymers and Composites,* Vol. 2, Marcel Dekker, New York, 1974.
18. P. J. Flory, *Principles of Polymer Chemistry,* Cornell University Press, Ithaca, NY, 1971.
19. C. W. Macosko and D. R. Miller, *Macromolecules,* **9,** 199 (1976).
20. C. Hepburn, *Polyurethane Elastomers,* Applied Science, London, 1982.
21. F. Hernandez-Sanchez and H. Vazquez-Torres, *J. Polym. Sci. Part A: Polym. Chem.,* **28,** 1579 (1990).

Received March 18, 1991
Accepted April 17, 1991